NORWEGIAN UNIVERSITY OF SCIENCE AND TECHNOLOGY
Faculty of Natural Science and Technology
Department of Materials Science and Engineering

Wettability of Silicon with Refractory Materials: A Review

ARJAN CIFTJA

MERETE TANGSTAD

THORVALD ABEL ENGH

Trondheim, February 2008

TABLE OF CONTENT

ABSTRACT

The wettability of ceramics by liquid metals is a key factor in many fields of high temperature materials science and engineering. The wetting behavior of liquid-silicon/refractory-materials system is especially important in refining and crystallization of silicon with respect to production of low cost solar cells but also in the production of silicon carbide based materials for advanced applications. This paper is a review on the wetting properties of molten silicon with various carbon, silicon carbide, silicon nitride and silica materials at high temperatures. Emphasis is given to reported data of the contact angles between molten silicon and ceramic substrates. The sessile drop method is the mainly used technique to determine the contact angles. A simple description of this method is also presented in this paper. In relation to chemical reaction between silicon and carbon with the formation of solid silicon carbide a model for the reaction kinetics and mechanisms is reported. Finally, the direction of future investigation of wettability of liquid-silicon with various refractory materials is proposed.

1. INTRODUCTION

The wettability of ceramics by liquid metals is a key factor in many fields of high temperature materials science and engineering [1]. During the last 10 years, considerable effort with respect to production of low cost solar cells has been directed at developing alternative processes for refining and crystallization of silicon. In these processes crucibles, dies, and substrates of various materials may be used. It is a prerequisite that the reactions with these refractory materials be kept to a low level so that the recontamination of the liquid silicon stays at a minimum [2].

Often graphite is used as a material for the production of crucibles and dies. At the graphite/silicon interface a layer of silicon carbide forms. Particles of silicon carbide in silicon have detrimental effects on the semiconductor properties and must be avoided [2]. Although some wetting experiments have been performed, a systematic and comprehensive investigation of the wetting behavior in the liquid-silicon/solid-carbon system is still lacking. The reason for this might be difficulties of studying the system, because wetting is

accompanied by chemical reaction between silicon and carbon with the formation of solid silicon carbide at the silicon/carbon interface, leading to an irreversible change in the physico-chemical nature of interface. Generally speaking, the wetting process in reactive metal/ceramic systems is controlled by the chemical reaction which takes place at the metal/ceramic interface. Consequently, analyses of reactive wetting require a more detailed understanding of the mechanism and kinetics of the interfacial reaction [3]. Silicon carbide, SiC, on the other hand is one of the silicon based ceramics, thus, the wettability of liquid-silicon/SiC-materials is reported by many authors [1, 4-6].

Silicon nitride (Si_3N_4) is another potential material for the production of solar cell grade silicon. The wetting behavior of Si_3N_4 is therefore of importance for the successful development of the technology. In addition, the wetting behavior in the system Si/Si_3N_4 is a critical parameter when infiltrating molten silicon into a reaction-bonded Si_3N_4 in order to obtain a dense material. Consequently, the wettability of this system has been investigated by many authors by the sessile drop method. However, different results have been reported because the wettability of Si/Si_3N_4 depends strongly on the experimental conditions [7].

Silicon single crystals are mainly produced by the Czochralski (CZ) method, in which silica is most commonly used as a crucible to hold the molten silicon. The wettability between SiO_2(s) and Si(l) plays an important role in CZ systems during crystal growth. However, few results have been reported because measurement is difficult in the liquid-silicon/solid-silica system [1].

The aim of this paper is to present the main results published concerning wettability of liquid-silicon/refractory-materials at high temperatures with the aim to show the areas where more careful investigation is needed.

2. METHODS AND TECHNIQUES

The wetting of a solid by a liquid drop is characterized by the contact angle, θ, defined in Figure 1 [8]. The experimental equipment used by most of the authors [1, 3-7, 9] to measure the contact angle by the sessile drop method consists essentially of a dense alumina tube whose central part is located inside a high-temperature furnace. Windows are fitted at each end of this tube; the drop on the substrate is illuminated by a high-intensity xenon lamp and can be photographed by a camera system. The tube is connected to a gas feed system and a vacuum device. The experiments are conducted in purified argon (purity of 99.998%) at a

pressure of one atmosphere [3-5, 9, 10]. The temperature is measured by a Pt/Pt+ 10% Rh thermocouple located in the immediate vicinity of the sample.

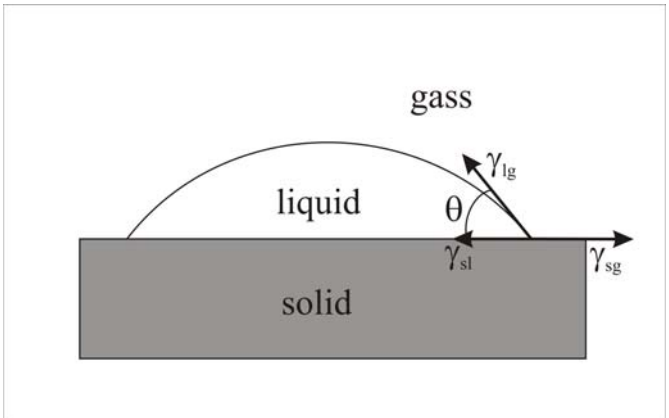

Figure 1: Contact angle θ of a liquid drop resting on a solid surface.

3. WETTABILITY OF SILICON WITH REFRACTORY MATERIALS

3.1 WETTING OF SOLID CARBON

Wettability and infiltration of molten silicon in carbon materials is widely studied. Silicon used in these studies has high purity (99.999%). Various types of carbon materials such as glassy or vitreous carbon, pyrolytic graphite, and natural graphites are employed as substrates with known open porosity and pore size [2, 3, 9-11]. After being polished with diamond pastes, the average surface roughness of the substrates R_a is measured. Surface roughness is the measure of the finer surface irregularities in the surface texture. These are the result of the manufacturing process employed to create surface. Surface roughness R_a is rated as the arithmetic average deviation of the surface valleys and peaks expressed in micrometers (see Figure 2) [12] and it is calculated by the following equation:

$$R_a = \frac{1}{l}\int_0^l \left| f(x) \right| \mathrm{d}x \qquad (1)$$

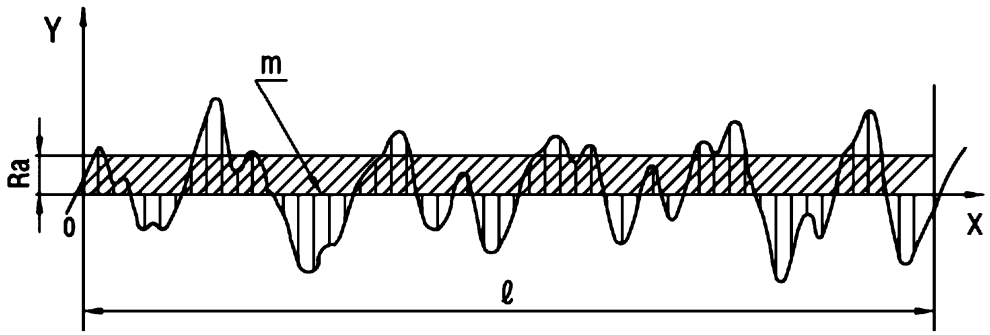

Figure 2: R_a is calculated as the arithmetic average of the peaks and valleys of the surface.

Melting (t = 0) starts at the contact points between the silicon and the substrate once the melting point (1414°C) of silicon is attained (Figure 3b). During melting the part of the silicon in the liquid state spreads on the substrate (Fig.3C) (Complete melting is usually achieved after 1.5 min). The contact angle θ generally takes relatively high values at the moment of the complete melting of the metal but decreases rapidly with time to stabilize at relatively low values after about 10 min [3].

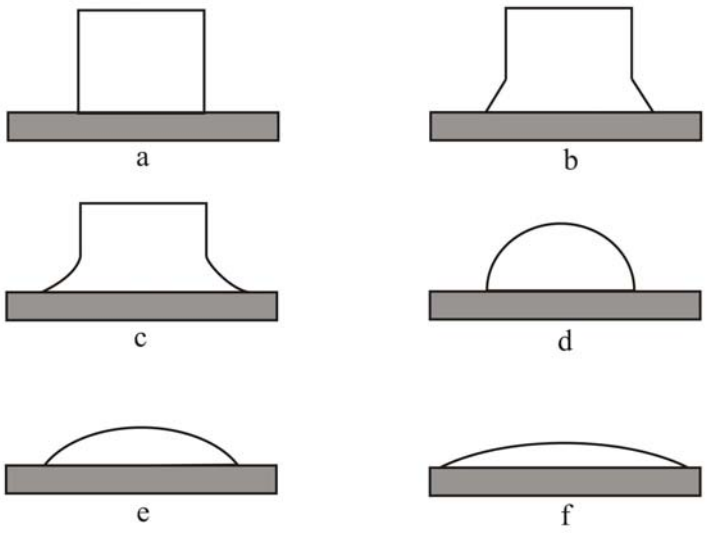

Figure 3: Schematic representation of melting process of silicon and its spreading on the graphite substrate. (a) before melting; (b) start of melting; (c) during melting; (d) complete melting; (e) during spreading and (f) stabilization [9].

Li and Hausner [9] used commercial graphite materials with different surface roughness as substrates and the contact angles were measured at 1430°C. The effect of substrate roughness

on the wettability in metal/ceramic systems has been the object of several studies. Wetting and flow in well-wetted (usually reactive) systems is enhanced by the roughening, while that of poorly wetted systems (non-reactive) is impeded by roughening [13]. As can be seen from Figures 4 and 5, surface roughening enhances the wetting of graphite materials by molten silicon.

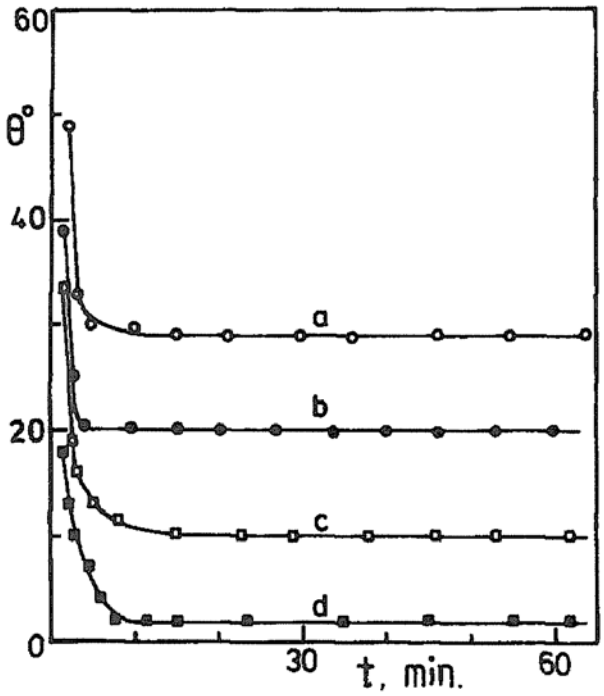

Figure 4: Time-dependent variation of the contact angle of silicon on graphite N with different surface roughness R_a. (a) R_a = 0.005 μm; (b) R_a = 0.30 μm; (c) R_a = 1.70 μm and (d) R_a = 3.18 μm.

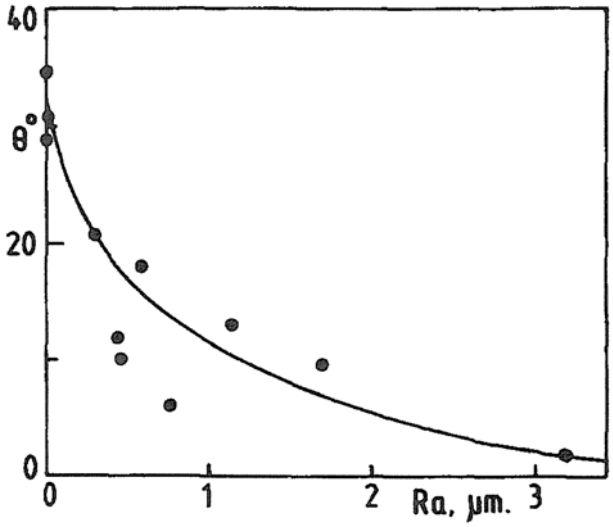

Figure 5: Stationary contact angle of silicon on graphite N as a function of substrate roughness R_a.

The infiltration of silicon into the graphite takes place within a depth noted by H. In addition, a lateral infiltration (see Figure 6) is observed, and the infiltrated distance measured from the solid-liquid-vapor three phase line is noted by D.

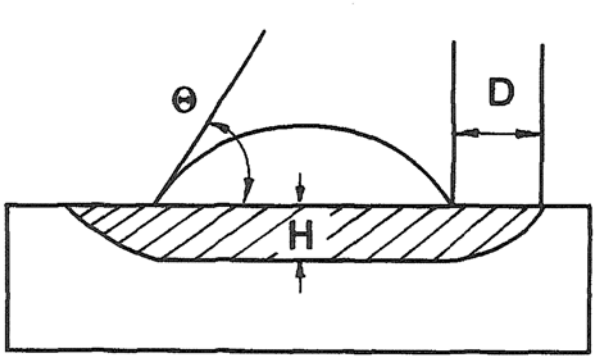

Figure 6: Schematic presentation of the cross-section of the silicon/graphite interface.

The measured values of H and D from a number of samples with different porosities and pore sizes are plotted in Figure 7 as a function of the stationary contact angles. The vertical infiltration depth H is about 0.9 ± 0.15 mm and seems to be independent on the contact angles. The vertical infiltration depth is different for different types of graphite materials (Table I). These results seem to indicate that the vertical infiltration depth increases as the porosity (or pore size) of the graphite materials is increased [9]. The lateral infiltration distance D increases as the contact angle θ decreases. Similar results were also achieved with other graphite materials. The obtained lateral infiltration distance-versus-contact angle relationship follows the curve shown in Figure 7.

Table I: Mean values of the open porosity, pore size of various graphite materials, and the vertical infiltration depth H (lower and upper limit values) of the materials by silicon.

Graphite	Porosity [%]	Pore size [μm]	Depth H [mm]
CB620	17.02	0.05	0.40 – 0.75
UT87	17.72	0.07	0.80 – 0.95
EK77	18.65	0.10	0.95 – 1.25
N	17.77	0.06	0.85 – 1.05

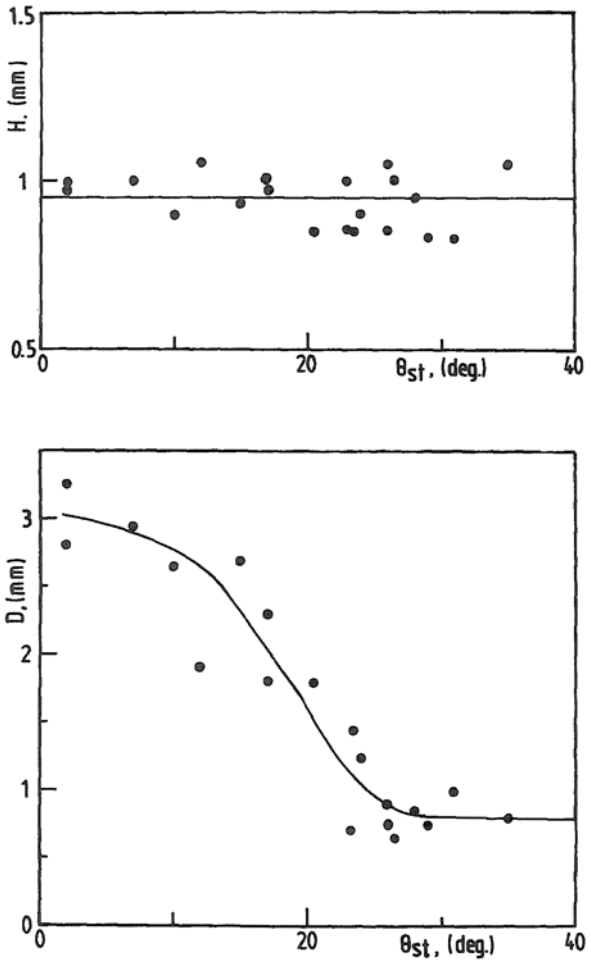

Figure 7: Vertical infiltration depth H and lateral infiltration distance D of silicon into the graphite N as a function of the stationary contact angles.

When glassy carbon substrates are used to study the wetting of molten silicon similar results compared to natural graphites are obtained. Wettability of glassy carbon materials with molten silicon is reported by several authors [2, 3, 9-11]. Li and Hausner [3] conducted two groups of wetting experiments. The first group refers to the experiments of *in situ* formation of sessile drops, as described above, where the silicon piece is placed on the substrate at room temperature and then heated to 1430°C. The second group refers to the experiments of the so-called capillary formation of sessile drops. In this case, the silicon sample is initially inserted into an alumina doser tube with a hole of 2 mm diameter in the side near the closed end of the tube. The metal sample inside the doser tube and the substrate are heated to 1430°C without being in contact. Once the temperature becomes constant, the liquid metal is forced out by an overpressure of argon through this orifice and descended about 1 cm directly onto the substrate to form the sessile drop. The purpose of such experiments is to avoid the reaction between liquid silicon and the carbon substrate during the melting process which takes place

in the experiments of *in situ* formation of sessile drops. In these experiments the surface roughness of the substrates were kept constant at R_a = 0.005 μm.

The results show that the measured contact angles are advancing angles. When the classical *in situ* formation of sessile drop technique is used, it is observed that the stationary contact angles depend on the silicon mass. Figure 8 shows the variation of contact angles with time for two different masses of silicon. In Figure 9 the stationary contact angle values are plotted as a function of the initial mass of silicon. There is a critical mass (about 60 mg) below which the contact angle decreases with a reduction in mass. Above this limit, the contact angle seems to increase slowly with the increase in mass. The maximal limiting contact angle that can be achieved with a large mass of silicon is about 40°. This value corresponds to the equilibrium θ value of liquid silicon on monocrystalline silicon carbide determined under the same experimental conditions [4, 5, 14].

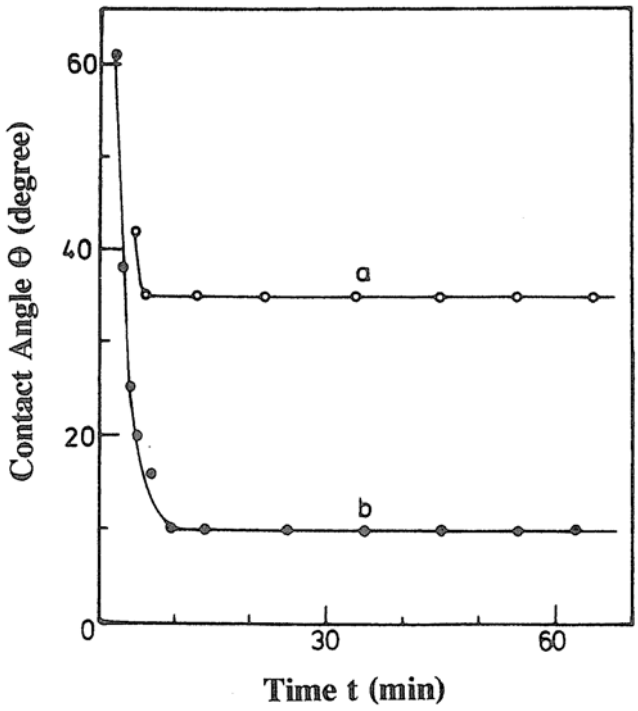

Figure 8: Time-dependent variations in the contact angles of liquid silicon on glassy carbon for different masses of silicon *M*: (a) *M* = 260 mg and (b) *M* = 18 mg.

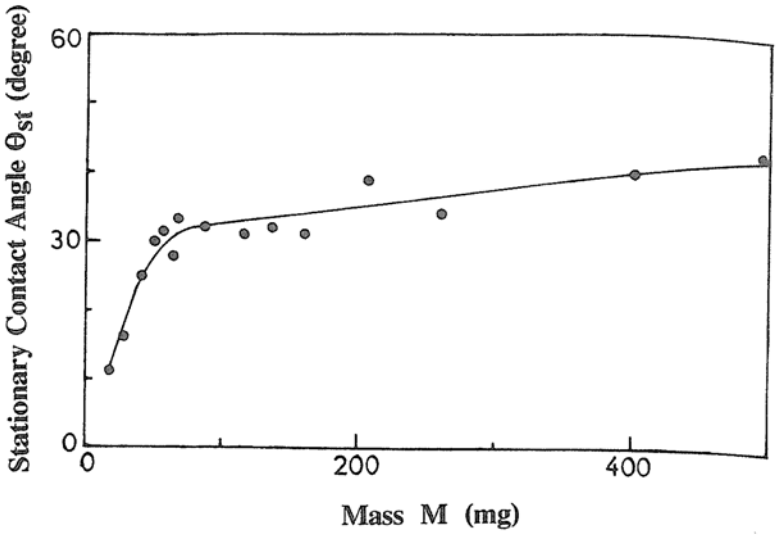

Figure 9: Stationary contact angles θ_{st} of liquid silicon on glassy carbon as a function of the mass of silicon M.

When the initial contact angles θ_{in} measured at the moment of complete melting of the metal are plotted against the stationary contact angles θ_{st} (or equilibrium contact angle), it is found that the stationary contact angle θ_{st} decreases with the increase in the initial contact angle θ_{in} (see Figure 10).

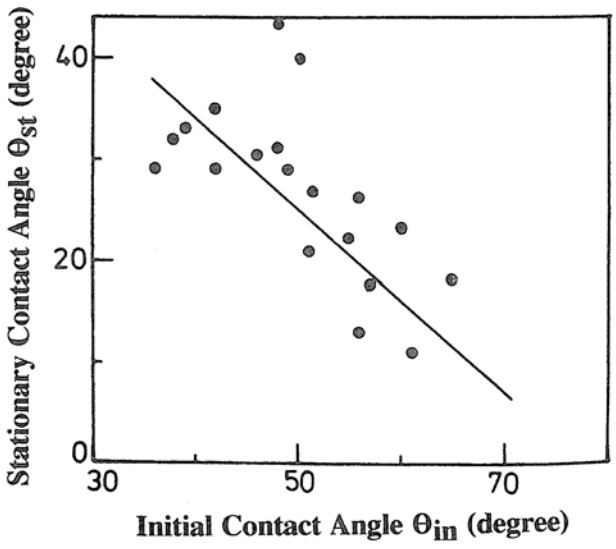

Figure 10: Stationary contact angle θ_{st} against the initial contact angle θ_{in} in the liquid-silicon/solid-glassy-carbon system.

Figure 11 shows the time-dependent variations in the contact angle of a *capillarily formed* liquid silicon drop on a glassy substrate. The contact angle initially takes a value of 95° ± 5° at the moment of the instantaneous formation (within a time less than 1 s) of the interface between the liquid metal the solid substrate, and then decreases with time to stabilize at about 10° after 20 to 40 min.

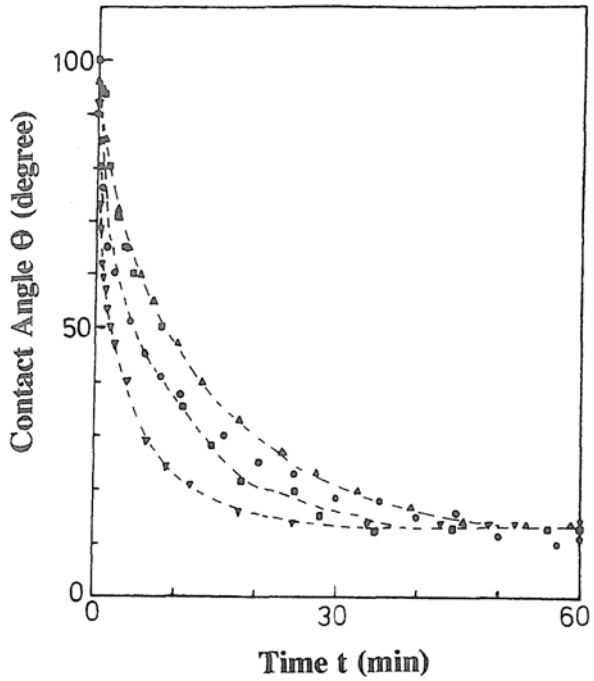

Figure 11: Time-dependant variations in the contact angle of capillarily formed pure liquid silicon drop on glassy carbon substrate (four independent experiments).

When capillarily formed liquid silicon pre-saturated with carbon is used, the results show that the contact angle takes an initial value of 120 ± 2° and then decreases with time to stabilize at about 10° after 10 min (Figure 12) [3].

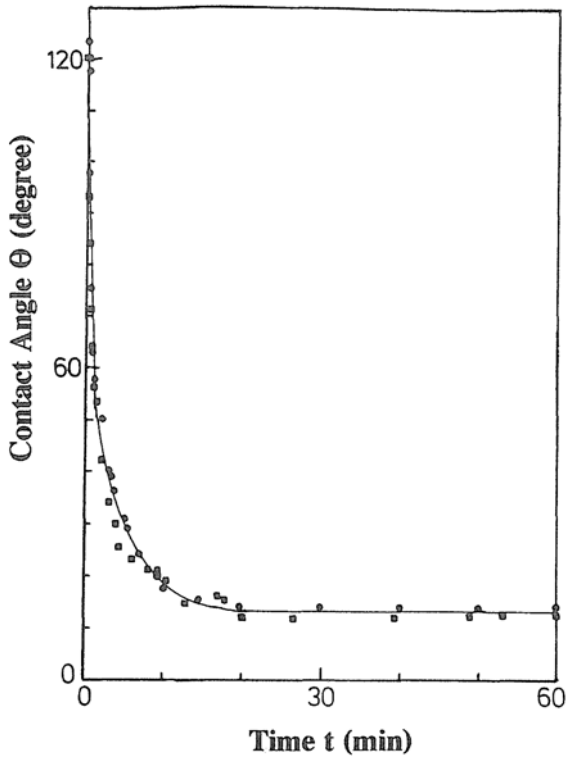

Figure 12: Time-dependant variations in the contact angle of liquid silicon pre-saturated with carbon on glassy carbon substrate (two independent experiments).

Dezellus *et al*. [11] performed wetting experiments with molten silicon on two different carbon materials: glassy (vitreous) carbon and pseudo-monocrystalline graphite. The average substrate roughness R_a was lower than 5nm on glassy carbon and about 2 – 4 nm for the pseudo-monocrystalline graphite. The pressure used in this study is 10^{-5} Pa. The measured initial contact angle is about 146° and the equilibrium contact angle of Si on glassy carbon was found to be 35°. The same results for the equilibrium contact angle are found on pseudo-monostrystalline graphite, but the measured initial angle was 120°. Experiments performed with silicon saturated with carbon showed the same result indicating that the *C* content of the liquid has no effect on θ_0.

Whalen and Anderson [14] reported equilibrium contact angles under vacuum at 1426°C from 40° to 50° for glassy carbon and 5 - 15° for graphite materials. Table II shows the summary of the results from various authors.

Table II: Equilibrium contact angles of liquid silicon on carbon materials. The average roughness R_a is indicated when reported by authors.

	Li and Hausner	Decellus	Whalen and Anderson	Naidich
Glassy carbon	10 - 40° (R_a < 0.005 μm)	36° (R_a = 5 nm)	40 - 50°	
Graphite	3° (R_a = 3.18 μm) 35° (R_a = 0.005 μm)	35 – 40° (R_a = 2 - 4 nm)	5 – 15° (pyrolytic graphite)	15°

3.2 WETTING OF SILICON CARBIDE

Wetting properties of molten silicon with silicon carbide materials have been shown great interest and widely studied by many authors. Nikolopoulos *et al*. [15] has employed the following SiC materials as substrates in their study:

(a) High-dense sintered α-SiC;

(b) α-SiC single crystals;

(c) β-SiC deposited by the CVD method on graphite substrate.

In situ formation of sessile drop technique measurements of the contact angle, θ, were carried out in a purified argon atmosphere. In the system SiC-Si with various silicon carbide substrates, a good wettability is observed and the contact angle is independent of annealing time (Figure 13). For mono- as well as polycrystalline α-Si the θ values are quite similar, i.e. about 38° at temperatures near the melting point of silicon. This value agrees reasonably well with results reported by Wahlen and Anderson [14] (40 ± 5° in vacuum at 1750 K) Naidich *et al*. [16] (36° in vacuum at 1750 K) and Yupko and Gnesin [17] (33 - 37° in vacuum at 1720 K). The same value for the contact angle is reported by Li and Hausner [4, 5] too (38° at 1703 K).

Some deviation from this value, i.e. 41.5°, is observed for the β-SiC [15]. This material was used as produced by the chemical vapor deposition (CVD) process with a roughness R_a = 0.5 μm.

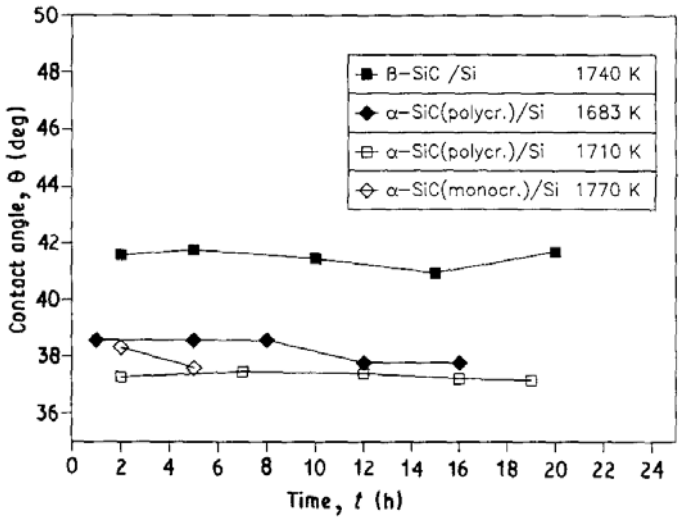

Figure 13: Time dependence of the contact angle for Si on various SiC substrates.

Mukai and Yuan [1, 6] reported a low value for the contact angle of 8° at 1693 K under argon gas ($P_{O2} \approx 10^{-21}$ MPa). The results for the contact angles for the Si(l)/SiC(s) are shown in Table III.

Table III: Contact angle of liquid silicon on SiC

Material	Temp [K]	θ [°]	Reference
α-SiC	1683 - 1770	38	Nikolopoulos
	1750	40 ± 5	Wahlen and Anderson
	1750	36	Naidich
	1720	33 – 37	Yupko and Gnesin
	1703	38	Li and Hausner
β-SiC	1740	41.5	Nikolopoulos
	1693	8	Mukai and Yuan

3.3 WETTING OF SILICON NITRIDE

Previous studies have shown that the wetting behavior in the Si(l)/Si_3N_4(s) system is very complex and depends considerably on the experimental conditions, probably due to the contamination of the silicon nitride surface by oxygen. A non-stoichiometric oxynitride layer on the silicon nitride surface was found to form quickly upon exposure to air even at room

temperature. Even at a low oxygen partial pressure, the contamination of the silicon nitride surface by oxygen has been proved to be inevitable. Li and Hausner [7] measured a value of about 50° for the contact angle measured in a neutral atmosphere. Swartz [18] observed that the wetting of reaction-bonded silicon nitride (RBSN) and chemical vapor deposition (CVD) Si_3N_4 by Si at 1430°C was a strong function of the inert gas pressure and found near-zero contact angles at low total pressures. The variation of θ with time has been observed also with sintered Si_3N_4 in argon and CVD Si_3N_4 substrates. Barsoum and Ownby [19] observed a small decrease in θ with decreasing oxygen partial pressure P_{O_2}, but with only for a quite limited range of P_{O_2}.

Li and Hausner [7] studied the influence of oxygen partial pressure on wetting behavior in the system Si(l)/Si_3N_4(s) over a large range of P_{O_2}. In their experiments the Si sample and the Si_3N_4 substrate were placed in a closed metal crucible. Different oxygen partial pressures can be obtained with different metals as the crucible material (Me = Fe, Mo, Ta, Ti and Zr). In this case the oxygen partial pressure inside the crucible is determined by the corresponding metal/metal oxide equilibrium oxygen pressure which can be calculated using thermodynamic data. If iron is used as crucible material, the drop of Si appears as being not molten completely at 1450°C. Only the part which has been in contact with the substrate seems to have been in the liquid state. The contact angle, θ, is estimated to be approximately 180° in this case. In the case of molybdenum, a symmetric Si drop has formed and a contact angle of about 53° has been observed. In both cases the surfaces of the silicon and Si_3N_4 substrate are strongly oxidized. When a tantalum, titanium or zirconium crucible is used the molten Si has a metallic appearance; in the case of zirconium, spreading has occurred. The measured contact angles at 1450°C and at a total pressure of 1 atm argon, together with those obtained by Barsoum and Ownby [19] at 1430°C and at a total pressure of 1 atm $H_2 + H_2O$ mixture are plotted in Figure 14 as a function of the oxygen partial pressure.

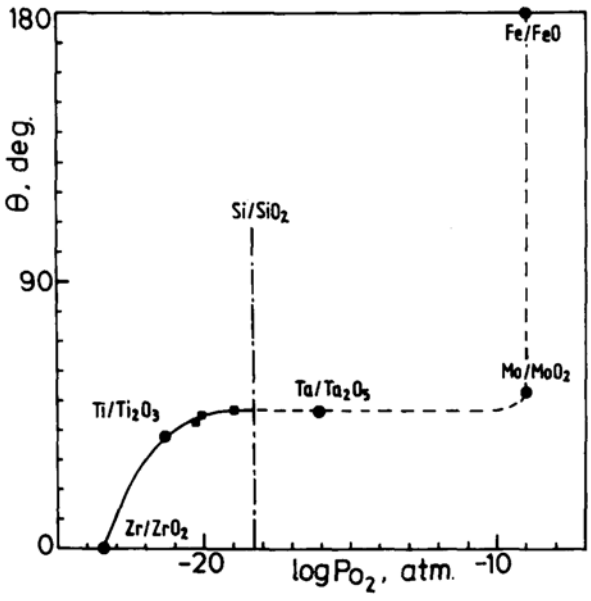

Figure 14: Contact angle θ in the system Si/Si_3N_4 as a function of oxygen partial pressure P_{O_2} at 1450°C. The points noted by (■) are the results obtained by Barsoum and Ownby with CVD Si_3N_4 substrates at 1430°C.

From Figure 14 it can be seen that the contact angle, θ, decreases sharply from 180° for the partially molten Si (Fe/FeO) to 53° (Mo/MoO_2). This sudden variation of θ around $Po_2 \approx 10^{-9}$ atm is attributed to the formation of a compact solid SiO_2 film. In the P_{O_2} range between 10^{-9} and 5.0 x 10^{-19} atm (Si/SiO_2), the contact angle, θ, remains practically constant ($\theta \approx 48°$). In the P_{O_2} range below 5.0x 10^{-19} atm up to 3.4 x 10^{-24} atm (Zr/ZrO_2), the contact angle is found to decrease with decreasing P_{O_2}. Complete wetting ($\theta = 0$) occurs when a strong oxygen getter such as zirconium (P_{O_2} = 3.4 x 10^{-24} atm) is present in the system. Yuan *et al.* conducted experiments under purified argon atmosphere with P_{O_2} in the range of 10^{-14} to 10^{-25} MPa. The contact angle at the beginning stage of the measurement gave 89° and gradually decreased with the elapsed time to a constant value of 85°. The decrease in contact angle during the initial period of the measurement may be caused by the dissolution of nitrogen from Si_3N_4 [2]. Since the value of nitrogen solubility in molten silicon at the melting point of silicon was around 4 mass ppm, the nitrogen concentration became steady and the contact angle stayed constant after 0.9 ks. Table IV shows the measured contact angles for the $Si(l)/Si_3N_4(s)$ system from various authors.

Table IV: Contact angle, θ, of molten silicon on various silicon nitride substrates

Substrate	Temperature [°C]	Atmosphere	θ [°]	Reference
Polycrystal	1500	Vacuum	< 40	Champion [20]
Sintered	1430	He	82 ± 3	O'Donnell [21]
	T.m.p.	Vacuum	134	Samsonov [22]
	1430	Ar	48 ± 3	Li and Hausner [7]
Hot-pressed	1427	Vacuum	43	Whalen and Anderson[14]
	1482		10	
	1430	He	50 ± 3	O'Donnell [23]
RBSN	-	Vacuum	< 10	Muller and Rebsch [24]
	1430	He	34 ± 2	O'Donnell [21]
			51 ± 2	
	1450	N_2	0	Inomata [25]
	1500	Vacuum	25	Messier [26]
	1670	Ar	10	Schmidt [27]
RBSN as received	1430	He	68 ~ 91	O'Donnell [21]
CVD	1450	He	~ 50	Duffy [28]
	1430	$H_2 \pm H_2O$		Barsoum and Ownby [19]
		$P_{O_2} = 1.1 \times 10^{-19}$atm	47	
		$P_{O_2} = 8.7 \times 10^{-21}$atm	45	
		$P_{O_2} = 6.0 \times 10^{-21}$atm	43	

3.4 WETTING OF SILICA

Due to the wide application in silicon production, wetting of silica substrates by molten silicon has shown great interest. However, limited results are reported because the measurement is difficult due to the high reactivity of the Si(l)/SiO2(s) system [6]. Yuan *et al*. [1] used silica substrate (99.98 mass% SiO_2) to measure the contact angle of molten silicon employing the sessile drop method. Figure15 shows the time variation of the contact angle between Si(l) and the SiO_2(s) plate at 1693 K. The contact angle at the beginning stage of the experiment is equal to 85° and decreases gradually with time.

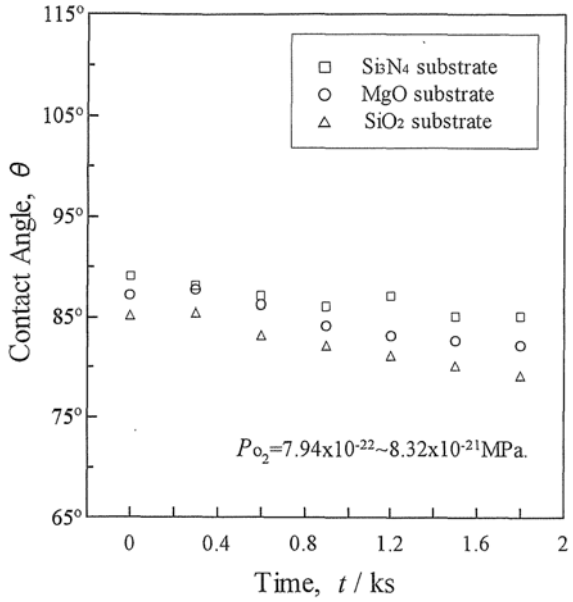

Figure 15: Time dependence of the contact angles of molten silicon on SiO_2, Si_3N_4 and MgO at 1693 K.

Nogi [29] measured the contact angle of Si(l)/SiO_2(s) system by the sessile drop method at 1723 K under an argon gas atmosphere (10^5 Pa) and reduced pressure (10^{-4} Pa). It was found that "the real contact angle" between Si(l) and SiO_2(s) is 80° and an apparent one is 95° at 1723 K. The difference between the real contact angle and the apparent one was stated to be caused by the evolution of SiO(g) gas at the interface between Si(l) and SiO_2(s).

Li and Hausner [4] used fused silica as a substrate and measured the contact angle of molten silicon at 1703 K. The results show that the contact angle has a value of 92° which remains constant during the 60 min of the experiment.

4. DISCUSION

4.1 LIQUID-SILICON/SOLID-CARBON SYSTEM

As shown in Table II there is an inconsistency in reported data for the contact angle of molten silicon on carbon substrates. The reported data can be divided in two groups: those that claim that the final contact angle of liquid-silicon/solid-carbon is at about 35° and those that claim that the final contact angle takes lower values of about 10 - 15°. According to Dezellus *et al*. [11] the wetting properties of molten silicon are sensitive to the oxygen partial pressure in the system. All of Li and Hausner's experiments are performed in an atmosphere of argon (purity of 99.998%) at a total pressure of 1 atm [3, 9] and such an atmosphere is characterized by a high oxygen partial pressure.

4.1.1 Reaction of molten silicon with glassy carbon materials

The microscopic observations (SEM) made on a cross section perpendicular to the interface reveal that, for the liquid-silicon/glassy-carbon interface, there are two distinct interfacial layers; both have been identified as SiC [3]. However, the first layer appears to be continuous with glassy carbon at the contact, while the second layer, which is located at the metal side of the interface, might be also discontinuous. The result strongly suggests that the second interfacial layer does not form during the holding period at 1430°C, but is produced by precipitation through a mechanism of the homogeneous nucleation and crystal growth from a supersaturated Si-C solution during the cooling period of the sample. Consequently, this layer has no effect on wetting, but may influence the mechanical properties of the interface.

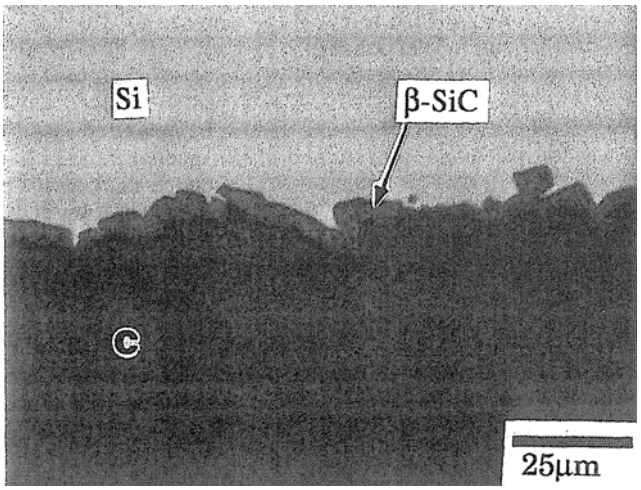

Figure 16: Microstructure of reaction formed SiC in the Si-C system at 1430°C.

From these observations it can be deduced that the reaction between liquid silicon and solid carbon proceeds mainly in two distinct stages [3]:

1. Dissolution of solid carbon in liquid silicon, which takes place instantaneously (within a time <1 s). Liquid silicon dissolves carbon and the diffusion of carbon in liquid silicon proceeds very quickly. Taking into account the strong interactions between Si and C, Si-C clusters might form in the liquid metal. Such clusters could preferentially adsorb at the liquid/solid interface to form an adsorption layer.

2. Once the adsorption layer is saturated by the Si-C clusters, the solid SiC could form through a combined process of the heterogeneous nucleation followed by crystal growth of a two-dimensional continuous SiC film at the liquid/solid interface. The initial formation of a continuous SiC layer with a thickness of few micrometers is produced during this precipitation process. After this linear regime of the SiC layer formation, the growth of the layer is slowed down, and further increase in the layer thickness is controlled by diffusion of the reaction species Si and C through this primarily formed SiC interfacial layer.

4.1.2 Infiltration of molten silicon into graphite materials

In contrary to glassy carbon materials the graphite materials have high porosity. Liquid silicon penetrates into the graphite and react to silicon carbide (SiC) in the pores. The open porosity is the main difference between graphites [9]. This difference is reflected in the depths of penetration which is ~1000 μm in a graphite with 11% porosity and ~200 μm in a graphite with 8% open porosity. At the interface between the graphite and the silicon the formation of the silicon carbide crystals began immediately after melting the silicon. During short reaction times, up to 20 min, the silicon carbide crystals grow nonuniformly in the form of islands [2].

However, as in the case of glassy carbon materials the silicon carbide formed in contact with graphite is present in two different morphologies.

1. One morphology exists at the interface with graphite and within the pores of the graphite. The silicon carbide particles are very fine and intimately associated with silicon.

2. The other morphology is found at the interface with the liquid silicon. Here, compact and large silicon carbide crystals are formed. Individual crystals may reach far into the silicon, or may even seem to be free being surrounded completely by the silicon phase. Often, there are spaces between neighboring crystals filled with silicon [2].

All the silicon carbide, the large crystals and the fine crystals in the first structure, consist of cubic β-silicon carbide.

4.1.2.1 Mechanism of formation of fine SiC inside the material

This structure, which is an intimate mixture of finely dispersed silicon carbide and silicon, is related to the porous structure of the carbon material. The structure of the graphites is nonuniform. There is a macrostructure consisting of large graphite particles and large pores. Each graphite grain has a microstructure with very fine graphite particles, often in the form of lamellae, and microporosity. It is believed that this structure forms in regions of high microporosity. The liquid silicon penetrates into such regions and reacts with the fine graphite lamellae to form fine silicon carbide. If the local graphite fraction is below a certain value (or the local porosity above a certain value) the silicon is not consumed by the reaction so that a silicon/silicon carbide mixture results [2, 10].

4.1.3 General considerations on reactive wetting

The wetting properties of solid ceramic materials by liquid metals are usually described by two quantities [13]:

a. The contact angle θ of a liquid metal (L) on a solid ceramic substrate (S) in vapor (V), related to the three σ_{ij} interfacial tensions by Young's equation:

$$\cos\theta = (\sigma_{SV} - \sigma_{SL}) / \sigma_{LV} \quad (1)$$

b. The work of adhesion W, that is, the work per unit area which should be provided to the system in order to separate reversibly a solid/liquid interface to create a solid/vapor interface and a liquid/vapor interface:

$$W = \sigma_{SV} + \sigma_{LV} - \sigma_{SL} \quad (2)$$

Taking into account Eq. (1), the work of adhesion W can then be written as

$$W = \sigma_{SV}(1 + \cos\theta) \quad (3)$$

According to Eq. (3), it is deduced that the wettability θ is determined by the adhesion energy W between the solid and the liquid contacting phases and by the cohesion energy $W_{coh} = 2\sigma_{LV}$ of the liquid phase.

The work of adhesion W in metal/ceramic systems is generally expressed as the sum of different contributions of the interfacial interactions between two phases [13]:

$$W = W_{equil} + W_{non\text{-}equil} \quad (4)$$

where W_{equil} represents the equilibrium contribution to the work of adhesion without chemical reaction at the metal/ceramic interface. $W_{non\text{-}equil}$ represents the nonequilibrium contribution to the work of adhesion when a chemical reaction takes place at the interface. This last contribution essentially affects the variation in the interfacial tension σ_{SL}, because the chemical reaction is taking place mainly in the interfacial region. In the case of an interfacial reaction accompanied by the formation of a new solid phase at the interface, the maximal lowering in the interfacial tension σ_{SL} has been proposed to be given by the following expression [3]:

$$\sigma_{SL} = \sigma_{SL}^{0} + d(\Delta G_R)/(d\Omega_{SL} \cdot dt) - \Delta\sigma_{SL} \qquad (\text{with } \Delta G_R < 0) \quad (5)$$

where σ_{SL} is the dynamic interfacial tension at the time t, and σ_{SL}^{0} is the initial interfacial tension at the time $t = 0$ without reaction. The second term on the right side of Eq. (5) represents the contribution of the free energy ΔG_R released by the interfacia1 reaction per unit area of interface $d\Omega_{SL}$ and per unit of time dt to the decrease in the interfacial tension. The last term takes into account the contribution of the change $\Delta\sigma_{SL}$ in the interfacial tension, which results from the *in situ* replacement of the initial metal/ceramic interface with at least one new interface after the reaction. Consequently, the importance of the kinetics of wetting comes into consideration. It should be noted that the role and relative importance of the free-energy term $d(\Delta G_R)/(d\Omega_{SL} \cdot dt)$ and of the interfacial tension term $\Delta\sigma_{SL}$ are system-dependent and may differ from one system to another [30].

Following the above considerations, the reactive wetting may be implicitly expressed as a function of different contributions:

$$\theta = \theta^{0} + f(d(\Delta G_R)/(d\Omega_{SL} \cdot dt), \Delta\sigma_{SL}, \ldots\text{etc}) \quad (6)$$

where θ is the dynamic contact angle and θ^{0} is the initial contact angle without reaction. In nonreactive systems, the contribution of interfacial reactions to wetting disappears, and the θ^{0} values can be directly determined by wetting experiments. In reactive systems, if the initial

contact angle θ^0 values are not known, they can be calculated by evaluating the equilibrium contribution of the work of adhesion W_{equil} according to:

$$\cos \theta^0 = (W_{equil}/\sigma_{LV}) - 1 \quad (7)$$

where σ_{LV} is the surface tension of the liquid metal. In metal/ceramic systems, W_{equil} may in turn be divided into two separate terms:

$$W_{equil} = W_{chem\text{-}equil} + W_{VDW} \quad (8)$$

$W_{chem\text{-}equil}$ is the cohesive energy between the two contacting phases, which results from the establishment of the chemical equilibrium bonds achieved by the mutual saturation (interfacial charge transfer) of the free valences of the contacting surfaces. The establishment of such chemical bonds is not accompanied by the rupture of the interatomic bonds in each of the contacting phases, which is taking place in chemical nonequilibrium systems. The second term in Eq. (8), W_{VDW} represents the energy of van der Waals interactions (dispersion force). In some cases, this energy can be numerically estimated, and the expression for the potential or dispersion interaction between a pair of atoms is usually used [3]:

$$E = -(3/2)(\alpha_1\alpha_2/R^6)[I_1I_2/(I_1I_2)] \quad (9)$$

where α_1 and α_2 are the polarizability volume; I_1 and I_2 the first ionization potential of atom 1 and 2, respectively. R is the distance between centers of the interacting atoms. If n is the umber of the interacting pairs per unit of interface, W_{VDW} is given by

$$W_{VDW} = -nE \quad (10)$$

4.1.4 Kinetics for wetting in liquid-silicon/solid-carbon system

A full understanding of the reaction kinetics and mechanisms is of great importance. However, there are only a few published data on the reaction kinetics, and the mechanisms are still far from being well understood. Fitzer and Gadow [31] proposed a diffusion mechanism and derived a mathematical model to describe the rate of growth of SiC, which was based on the mass balance among the various mass transfer processes, such as mass transfer through the boundary layer in molten silicon, mass diffusion across the solid SiC layer, and reaction at the SiC/Si interface.

Zhou and Singh [10] placed emphasis on investigation of the reaction kinetics and mechanisms in the Si-C reaction over a temperature range of 1430° to 1510°C. They studied the reaction kinetics of liquid silicon with solid carbon using a variety of carbon materials such as polycrystalline graphite, pyrolytic graphite and glassy carbon. The results of the reaction of liquid Si with polycrystalline graphite showed that liquid silicon physically penetrated into the pores of the graphite and reacted with the graphite. Once the surface pores

of the graphite were closed upon the formation of SiC, the penetration of liquid silicon stopped, but the reaction carried on to make this layer grow due to the diffusion of reactants through the reaction-formed SiC barrier layer. Obviously, two conceptually independent processes of infiltration and reaction were involved in this reaction. In practice, however, these two processes were not separable at the temperature of this study, which made it impossible to study only the kinetics of the Si-C reaction. Therefore, these graphitic materials are not suitable for studying reaction kinetics.

Glassy carbon plates with a density of 1.42 g/cm^3 is a material chosen as a carbon source for the kinetics study to react with a pure Si melt. This material is nonporous in microrange, though it contains a number of very fine voids of 1 to 3 nm in diameter.

The variation in the thickness of the reaction-formed SiC layer with exposure time is used as a measure of the reaction kinetics. The average thickness is determined by dividing the SiC area in the polished cross section by the length of a line parallel to the SiC/C interface [10, 32].

The reaction of carbon with silicon to form SiC can take place almost immediately after the solid carbon sample is immersed into molten silicon at a temperature slightly above the melting point of silicon. A continuous solid SiC layer is formed on the original surface of carbon, thereby preventing the molten silicon from directly contacting carbon, so that either silicon or carbon has to diffuse through the SiC layer to sustain the reaction. Since the reaction of carbon with the silicon melt proceeds extremely fast compared to the diffusion in solid, the diffusion of the silicon and/or the carbon is considered to be the rate-limiting step for the whole process. The SiC layer becomes thicker and more uniform with increasing reaction time. Neither an increase in the reaction temperature within a range of 1430° to 1510°C nor an extension in the reaction time can fundamentally change the microstructural morphology of the reaction- formed and continuous SiC layer. The exact reaction product morphology may depend on the type of carbon precursor used.

The overall reaction rate for the Si-C reaction is plotted in Figure 17 as the average thickness of the continuous SiC layer vs exposure time at 1430°, 1475°, and 1510°C. The growth rate of the continuous SiC layer obeys a fourth-power rate law for the reaction of glassy carbon with a pure Si melt.

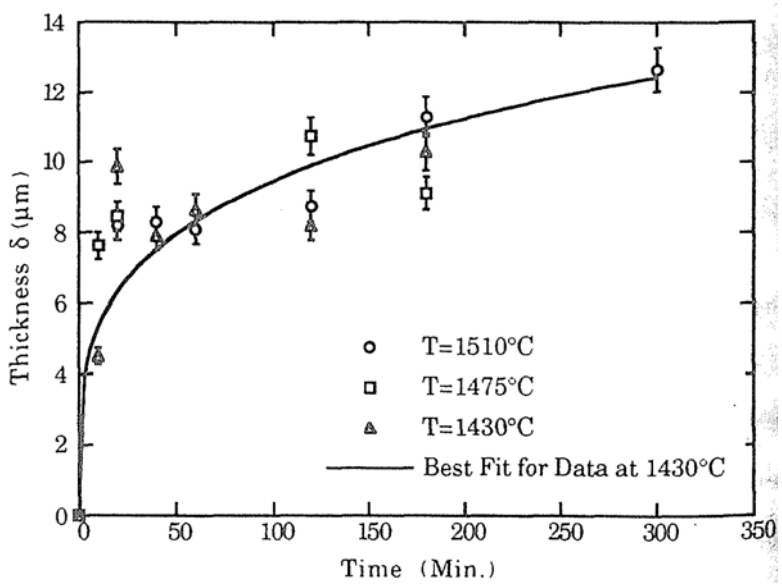

Figure 17: Thickness of the SiC layer as a function of the reaction time for Si-C reaction at 1430°, 1475°, and 1510°C [10].

The fourth-power rate law can be expressed as:

$$\delta = kt^{1/4}$$

where δ is the average thickness of the continuous SiC layer, t is the reaction time, and k is a constant. In the temperature range of 1430° to 1510°C, k is almost always equal to 3 for the Si-C system, which indicates that the processing temperature of this study has little influence on the reaction kinetics [33]. This might be due to the exothermic reaction between solid carbon and molten silicon in which a large amount of the heat of reaction will be given off so that the local temperature near the reaction front will be increased.

4.1.4.1 A model for reaction kinetics

Here we present a model developed by Zhou and Singh [10] that tries to explain the growth rate of SiC from the reaction of glassy carbon with a pure silicon melt.

In the temperature range of 1430° to 1510°C a considerable concentration of lattice and/or electronic defects could exist in the reaction-formed SiC. Because of the lower electron affinity of the chemisorbed silicon, the silicon would give an electron to the SiC layer with a simultaneous formation of the silicon ion at the Si/SiC interface,

$$Si \leftrightarrow Si^{+} + e^{-} \qquad (11a)$$

whereas at the SiC/C interface, carbon would be ionized by obtaining an electron, that is,

$$C + e^{-} \leftrightarrow C^{-} \qquad (12)$$

The ionization to higher degree requires higher energy, so only the ionization to first degree will happen in this case. Since the self-diffusion of either silicon or carbon in the β-SiC occurs via a vacancy mechanism [34], we can rationally assume that the major lattice defects in the β-SiC layer are of Schottky type, that is, the carbon-ion vacancy with the positive charge (z = 1) and silicon-ion vacancy with the negative charge. Because of the much faster self-diffusion of carbon in β-SiC in comparison to silicon, another reasonable assumption is that the growth rate of the SiC layer is controlled by the diffusion of carbon-ion vacancy with electrons so that the electric charge neutrality of the materials can be maintained.

β-SiC has the zinc blend crystal structure and its lattice parameter is equal to 4.387 Å at 1783 K as obtained by means of linear extrapolation. From this information, the total number of carbon ions in β-SiC, $N = 4.73 \times 10^{22}$ cm^{-3}, is calculated. Since the lattice defects are of Schottky type, the concentration of the carbon-ion vacancy, n_{vc}, can be described by the following equation:

$$n_{vc} = N \exp\left(-E_{vc} / kT\right) \tag{13}$$

where E_{vc} is the energy expended in creating a vacancy and is approximately equal to 6 eV. So we get $n_{vc}^{1783} = 5.38 \times 10^5$ cm^{-3} at T = 1783 K. In addition, the concentration of the intrinsic electrons in the conduction band of β-SiC at 1783 K, $n_e^{1783} = 1.70 \times 10^{18}$ cm^{-3}, can also be obtained by linear extrapolation. It is obvious that the concentration of electrons in the β-SiC layer is much larger than the carbon-ion vacancy concentration, i.e., $n_e >> zn_{vc}$, which should cause a negative space charge. In the first approximation, we can assume that

$$n_e = azn_{vc} \tag{14}$$

where a is a constant and obviously much greater than unity.

Since Si is in a sufficient amount for the reaction, the electron concentration at the phase boundary of Si/SiC is kept constant by the inexhaustible electron supply of the Si phase. According to Eq. (14), the concentration of carbon-ion vacancies at the Si/SiC interface (x = 0), n_{vc}^0, should also be constant, i.e.,

$$n_{vc} = n_{vc}^0 \qquad (\text{at } x = 0) \tag{15a}$$

In addition, the concentrations of the carbon-ion vacancies and electrons should decrease continuously from the Si/SiC interface to the SiC/C interface (x = δ), since the corresponding chemical equilibrium is assumed at both interfaces. The concentration profile and the flux direction of these defects are shown in Figure 18. It is similar to the oxidation model by Hauffe [35], in which a positive space charge was present instead of a negative space charge

in the Si-C reaction. In this oxidation model, the concentration of lattice defects at any instant of oxide growth is found to decrease exponentially in comparison to the concentration of lattice defects at the surface of metal (x = 0). It is reasonable to assume that the carbon-ion vacancies in our case distribute across the space charge layer of SiC in the same manner as in the case of the oxidation described above. Thus, the concentration of carbon-ion vacancies decreases from the Si/SiC interface to the SiC/C interface exponentially. As a consequence, the concentration at the Si/SiC interface is much higher than that at the SiC/C interface, n_{vc}^{δ}, i.e.,

$$n_{vc}^{0} >> n_{vc}^{\delta} \tag{15b}$$

Furthermore, the electric potential should also be independent of the thickness of the SiC layer because a chemical equilibrium is established at both interfaces, which leads to the boundary conditions given below:

$$V^{0} = 0 \qquad \text{(at x = 0)} \tag{16a}$$

$$V^{\delta} = 0 \qquad \text{(at x = } \delta\text{)} \tag{16b}$$

where V^{0} is a constant electric potential at the SiC/C interface with respect to the SiC/Si interface.

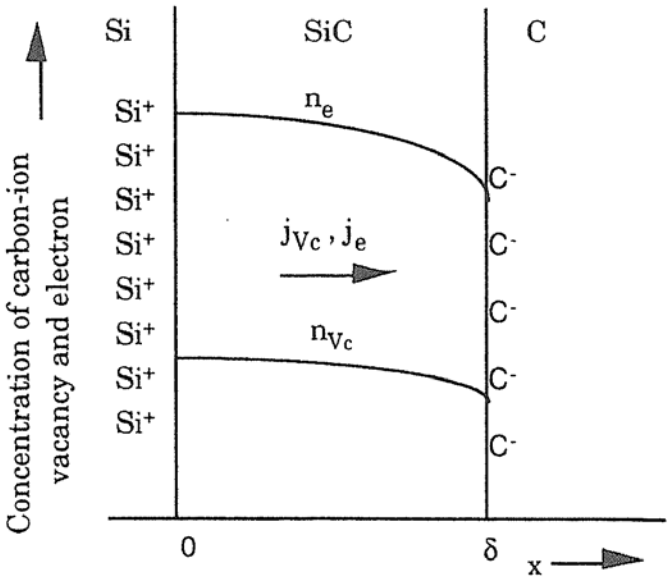

Figure 18: Concentration profiles and diffusion flux of carbon-ion vacancies and electrons [10].

The flux of carbon-ion vacancies, j_{vc}, can be written as:

$$j_{vc} = -D\frac{dn_{vc}}{dx} - zen_{vc}B\frac{dV}{dx} \tag{17}$$

where D and B are the diffusion coefficient and mobility of carbon-ion vacancies, respectively, x denotes the coordinate perpendicular to the original of a carbon sample, and V is the electrical potential across the SiC layer. The flux of electrons can also be described by a similar equation. Both relations have to be combined with the Poisson equation:

$$\frac{\mathrm{d}^2V}{\mathrm{d}x^2} = -\frac{1}{\varepsilon\varepsilon_0}(n_\mathrm{e} - zn_\mathrm{vc})e \tag{18}$$

where e is the elementary charge, ε_0 the permittivity of free space, and ε the dielectric constant of β-SiC.

Substituting Eq. (14) into Eq. (18) and knowing that the value of a is much greater than unity, the Poisson equation can be rewritten as:

$$\frac{\mathrm{d}^2V}{\mathrm{d}x^2} = -\frac{azen_\mathrm{vc}}{\varepsilon\varepsilon_0} \tag{19}$$

As discussed above, the growth rate of the SiC layer is determined by the diffusion of carbon-ion vacancies across the SiC layer. Therefore, we get Eq. (20) for the relationship between the growth rate of the SiC layer and the flux of the carbon-ion vacancies as follows:

$$j_\mathrm{vc} = n_\mathrm{vc}^{\delta} \cdot \frac{\mathrm{d}\delta}{\mathrm{d}t} \tag{20}$$

We assume that the diffusion of carbon-ion vacancies from the Si/SiC interface to the SiC/C interface is driven predominately by the electric field, i.e.,

$$j_\mathrm{vc} = -zen_\mathrm{vc}B\frac{\mathrm{d}V}{\mathrm{d}x} \tag{21}$$

and the growth of SiC layer for quasi-steady state is:

$$\frac{\mathrm{d}j_\mathrm{vc}}{\mathrm{d}x} = 0 \tag{22}$$

Differentiating Eq. (21) and substituting into Eq. (22) we obtain:

$$\frac{\mathrm{d}n_\mathrm{vc}}{\mathrm{d}x}\frac{\mathrm{d}V}{\mathrm{d}x} + n_\mathrm{vc}\frac{\mathrm{d}^2V}{\mathrm{d}x^2} = 0 \tag{23}$$

Substituting Eqs. (19) and (21) into Eq. (23) yields

$$\frac{\mathrm{d}n_\mathrm{vc}}{\mathrm{d}x} = -\frac{\alpha}{2}n_\mathrm{vc}^3 \tag{24}$$

where $\alpha = \dfrac{2a(ze)^2B}{j_\mathrm{vc}\varepsilon\varepsilon_0}$

Integration of Eq. (24) with the limiting condition (15a) yields

$$n_{vc} = \frac{1}{(\alpha x + (1/n_{vc}^0)^2)^{1/2}} \tag{25}$$

Substituting Eq. (25) into Eq. (21), we get

$$\frac{dV}{dx} = -\frac{j_{vc}}{zeB}(\alpha x + (1/n_{vc}^0)^2)^{1/2} \tag{26}$$

Integrating Eq. (26) with the boundary condition (16a), we obtain

$$\beta V = (\alpha x + (1/n_{vc}^0)^2)^{3/2} - (1/n_{vc}^0)^3 \tag{27}$$

where

$$\beta = -\frac{3ze}{2j_{vc}}\alpha B = -\frac{3a(ze)^3 B^2}{j_{vc}^2 \varepsilon\varepsilon_0}$$

Substituting another boundary condition (16b) into Eq. (27), we get

$$\beta V_0 = (\alpha\delta + (1/n_{vc}^0)^2)^{3/2} - (1/n_{vc}^0)^3 \tag{28}$$

This equation gives the relationship between the carbon-ion vacancy flux j_{vc} and other parameters such as the concentration n_{vc}^0, the mobility B, and the potential V_0.

Substituting x = δ into Eq. (25), Eq. (25) can be rewritten as follows:

$$(\alpha\delta)^{-1/2} = \frac{n_{vc}^0}{\sqrt{(n_{vc}^0)^2 - (n_{vc}^\delta)^2}} n_{vc}^\delta \tag{29}$$

Since $n_{vc}^0 >> n_{vc}^\delta$, Eq. (29) can be simplified to

$$(\alpha\delta)^{-1/2} \approx n_{vc}^\delta$$

and then we have due to Eq. (15b)

$$n_{vc}^0 >> (\alpha\delta)^{-1/2} \tag{30}$$

Equation (30) is equivalent to the relation

$$\alpha\delta >> (1/n_{vc}^0)^2$$

Therefore, Eq. (28) is modified to

$$\beta V_0 = (\alpha\delta)^{3/2} \tag{31}$$

Substitution of α and β into Eq. (31) yields

$$j_{vc} = \frac{9\varepsilon\varepsilon_0 B V_0^2}{8a} \cdot \frac{1}{\delta^3} \tag{32}$$

Finally, by substitution of the relationship between the flux j_{vc} and the growth rate $d\delta/dt$ given by Eq. (20), the fourth-power rate law in the form of differential equation is obtained as follows:

$$\frac{\mathrm{d}\delta}{\mathrm{d}t} = \frac{k_0}{4}\frac{1}{\delta^3} \tag{33}$$

where

$$k_0 = \frac{9}{2}\frac{V_0^2}{an_{\mathrm{vc}}^{\delta}} B\varepsilon\varepsilon_0 \tag{34}$$

which is in a good agreement with the results of regression analysis of the experimental data.

In order to make direct comparison of this model with experimental data, we integrate Eq. (33) with $\delta = 0$ when $t = 0$ and get

$$\delta^4 = k_0\, t \tag{35}$$

or

$$\delta = k_0^{1/4} t^{1/4} \tag{36}$$

With the aid of the Nernst-Einstein equation, $D = Bk_{\mathrm{B}}T$ (k_{B} is Boltzmann's constant) and Eq. (14), we can obtain an equation for calculating the variation of thickness of SiC with reaction time as follows:

$$\delta = \left(\frac{9}{2}\frac{\varepsilon\varepsilon_0 z V_0^2}{k_{\mathrm{B}}T}\frac{D}{n_{\mathrm{e}}^{\delta}}\right)^{1/4} t^{1/4} \tag{37}$$

where n_{e}^{δ} is the electron concentration at the SiC/C interface. At T = 1510°C, V_0 is equal to -2.02 V, and boundary diffusion coefficient of carbon can be calculated by extrapolating data from the published literature [34], i.e., $D_{\mathrm{bc}} \approx 1.43 \times 10^{-9}$ cm^2/s. Since the electron concentration at the SiC/C interface is unknown, we use the equilibrium concentration of electrons in the SiC layer, i.e., $n_{\mathrm{e}}^{1783} = 1.70 \times 10^{18}$ cm^{-3}, instead of n_{e}^{δ} to calculate the thickness of SiC at different reaction times. This calculated thickness of SiC layer, as a function of reaction time, is plotted in Figure 19 together with the corresponding experimental data and best fit to the fourth-power rate law. The calculated curve using Eq. (37) is much below the experimental values. However, if we multiply this calculated curve by 4 and replot the curve, it becomes amazingly close to the experimental curve at 1510°C. This discrepancy by a factor of 4 can be attributed to the use of the equilibrium concentration in calculating the theoretical curve, which will underestimate the thickness values because the equilibrium concentration should be higher than the concentration at the SiC/C interface.

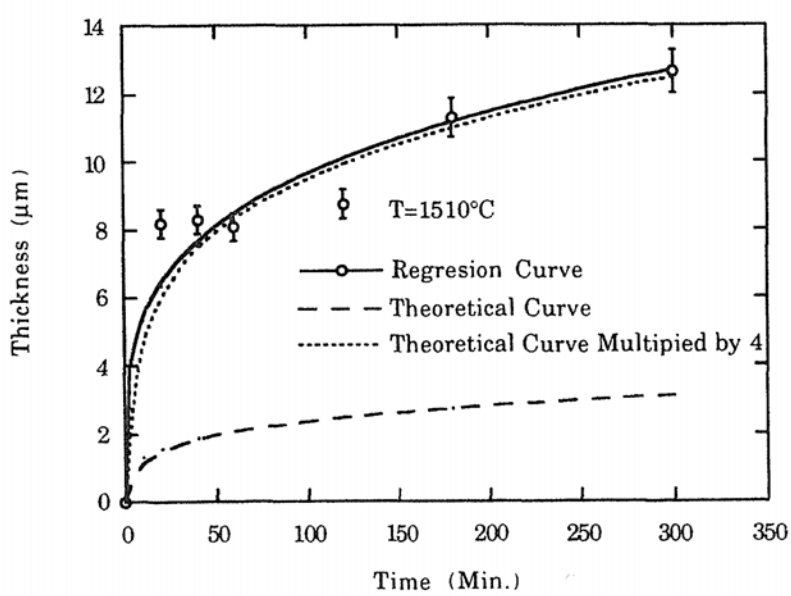

Figure 19: Comparison of the theoretical curve with experimental data of Si-C reaction at 1510°C.

4.2 LIQUID-SILICON/SILICON-NITRIDE SYSTEM

As shown before the wetting behavior in Si(l)/Si_3N_4(s) system is very complex and depends considerably on the experimental conditions, due to the contamination of the silicon nitride surface by oxygen. The interaction between oxygen and Si_3N_4 leads to the formation of a non-stoichiometric oxynitride SiO_xN_y layer on the Si_3N_4 surface. The thickness of this layer is reported to be about 3 nm. The composition of the SiO_xN_y layer can vary over a large range depending on the oxygen concentration which in turn depends on the experimental conditions of the Si_3N_4 deposition. In contact with Si, the oxygen in the SiO_xN_y layer can be eliminated by reaction between Si and SiO_xN_y, leading to the formation of a gaseous species, SiO:

$$4\ SiO_xN_y + [3y + 4(x\text{-}1)]Si \leftrightarrows y Si_3N_4 + 4x SiO \qquad (38)$$

The elimination of oxygen will increase with temperature and with decreasing total pressure and oxygen partial pressure.

It is interesting to note that the observations of Duffy *et al*. [28] indicate that the contact angle of molten Si on oxynitride layers in helium is initially high but decreases with time as the oxynitride layers are converted to β-Si_3N_4 according to reaction (38).

SUMMARY

The sessile drop method is used to measure the contact angles of liquid silicon with various substrates at different experimental conditions. The substrates are carbon materials, silicon carbides, silicon nitrides and silica.

Wetting and flow in well-wetted systems is enhanced by the roughening. When graphites are used as substrates infiltration of silicon into the graphite material takes place. The infiltration depth increases as the porosity (or pore size) of the graphite materials is increased.

From the discussion on the characteristic contact angles it is clear that pure Si does not wet an unreacted carbon surface, and that good wetting is obtained because of the formation of a continuous layer of SiC at the liquid-silicon/solid-carbon interface. The rate at which the Si droplet spreads is limited by the rate of the interfacial reaction (to form SiC) itself. The final contact angle of molten silicon in carbon materials is reported to be about 35° which corresponds to the contact angle of molten silicon on silicon carbide substrate.

The studies have shown that the wetting behavior in $Si(l)/Si_3N_4(s)$ system is very complex and depends considerably on the oxygen concentration in the system, due to the contamination of the silicon nitride surface by oxygen. Thus, for the contact angle of molten silicon on silicon nitride materials values from about 85° to 10° are reported. At very low oxygen partial pressures in the region of about 10^{-24} atm complete wetting can be achieved at 1450°C.

A contact value of about 90° is reported for wetting of molten silicon on silica substrate.

FUTURE WORK

Although considerable work is carried out on studying the wettability of molten silicon with various substrates, still further research is needed. As mentioned, wetting in this case is accompanied by a chemical reaction between silicon and the substrate material thus making it difficult to measure the real contact angle which varies with time.

Kinetics of the chemical reaction is an important factor which defines the spreading of the molten silicon on the substrate surface and the variation of contact angle with time. A few efforts have been made to develop an acceptable kinetics theory in the solid-carbon/liquid-silicon system but with little success so far. Therefore, investigation of wettability kinetics is important.

As mentioned in the literature survey, pure solar grade silicon with impurities < 1ppm is used to measure the wettability with refractories. In the processes of refining metallurgical grade silicon (MG-Si) to solar grade silicon (SoG-Si) it is the wettability of MG-Si that requires special interest. Impurities in the feedstock and during the refining steps dominate over those in the SoG-Si. They affect the wettability of molten silicon with refractories. Thus, research on the effect of various impurities on wettability of silicon is important.

REFERENCES

1. Yuan, Z., W.L. Huang, and K. Mukai, *Wettability and reactivity of molten silicon with various substrates.* Applied Physics A – Materials Science & Processing, 2004. **78**: p. 617–622.

2. Deike, R. and K. Schwerdtfeger, *Reactions between liquid silicon and different refractory materials.* Journal of Electrochemical Society, 1995. **142**(2): p. 609-614.

3. Li, J.-G. and H. Hausner, *Reactive Wetting in the Liquid-Silicon/Solid-Carbon System.* Journal of American Ceramic Society, 1996. **79**(4): p. 873-880.

4. Li, J.G. and H. Hausner, *Wetting and adhesion in liquid silicon/ceramic systems* Materials Letters, 1992. **14**: p. 329-332

5. Li, J.G. and H. Hausner, *Wettability of silicon carbide by gold, germanium and silicon* Journal of Materials Science Letters, 1991. **10**: p. 1275-1276.

6. Mukai, K. and Z. Yuan, *Wettability of ceramics with molten silicon at temperatures ranging from 1693 to 1773 K.* Materials Transactions, JIM, 2000. **41**(2): p. 338-345.

7. Li, J.G. and H. Hausner, *Influence of Oxygen Partial Pressure on the Wetting Behaviour of Silicon Nitride by Molten Silicon.* Journal of the European Ceramic Society, 1992. **9**: p. 101-105.

8. Stølen, S. and T. Grande, *Surfaces, Interfaces and Adsorbtion*, in *Chemical Thermodynamics of Materials: Macroscopic and Microscopic Aspects*. 2004, John Wiley and Sons Ltd. p. 171-172.

9. Li, J.-G. and H. Hausner, *Wetting and infiltration of graphite materials by molten silicon.* Scripta Metallurgica *et* Materialia, 1995. **32**(3): p. 377-382.

10. Zhou, H. and R.N. Singh, *Kinetics Model for the Growth of Silicon Carbide by the Reaction of Liquid Silicon with Carbon* Journal of American Ceramic Society, 1995. **78**(9): p. 2456-2462.

11. Dezellus, O., et al., *Wetting and infiltration of carbon by liquid silicon.* Journal of Materials Science, 2005. **40**: p. 2307–2311.

12. Edge, E. *Surface Texture / Roughness*. 2000-2008 [cited; Available from: http://www.engineersedge.com/surface_finish.htm.

13. Naidich, Y.V., *The wettability of solids by liquid metals.* Progress in Surface and Membrane Science, 1981. **14**: p. 353-484.

14. Whalen, T.J. and A.T. Anderson, *Wetting of silicon carbide, silicon nitride, and carbon by silicon and binary silicon alloys.* Journal of the American Ceramic Society, 1975. **58**(9-10): p. 396-399.

15. Nikolopoulos, P., et al., *Wettability and interfacial energies in SiC-liquid metal systems.* Journal of Materials Science, 1992. **27**: p. 139-145.

16. Naidich, Y.V., V. Zhuravlev, and N. Krasovskaya, *The wettability of silicon carbide by Au – Si alloys.* Materials Science and Engineering A, 1998. **245**: p. 293–299.

17. Yupko, V.L. and G.G. Gnesin, *Contact interaction of silicon carbide with liquid silicon.* Poroshkovaya Metallurgiya, 1973. **13**(10): p. 97-101.

18. Swartz, J.C., *Atmosphere effects on wetting of Si3N4 by liquid Si.* Journal of American Ceramic Society, 1976. **59**: p. 272-273.

19. Barsoum, M.W. and P.D. Ownby, *The effect of oxygen partial pressure onwetting of SiC, AlN and Si3N4*, in *Surfaces and Interfaces in Ceramic and Ceramic-Metal Systems*, P.J. A. and A. Evans, Editors. 1981. p. 457-466.

20. Champion, J.A., B.J. Keene, and S. Allen, *Wetting of refractory materials by molten metallides.* Journal of Materials Science, 1973. **8**(3): p. 423-426.

21. O'Donnell, T., M. Leipold, and M. Hagan, *Compatibility studies of various refractory materials in contact with molten silicon*, in *DOE/JPL/1012-77/6, JPL-PUB-78-18*. 1978.

22. Samsonov, G.V. and I.M. Vinitzkii, *Handbook of Refractory Compounds*, ed. IFI/Plenum. 1980, New York, USA.

23. Leipold, M.H., T.P. O'Donnell, and M.A. Hagan, *Materials of construction for silicon crystal growth.* Journal of Crystal Growth, 1980. **50**(1): p. 366-377.

24. Mueller, K. and H. Rebsch, *Silicon nitride; corrosion and aluminum resistant.* Silikattechnik, 1966. **17**(9): p. 279-282.

25. Inomata, Y., *Oxidation resistant Si-impregnated surface layer of reaction sintered nitride articles.* Yogyo-Kyokai-Shi, 1975. **83**: p. 1-3.

26. Messier, D.R., *Use of Ti to enhance wetting of reaction-bonded Si3N4 by Si.* Ceramic Engineering and Science Proceedings, 1980. **1**: p. 624-633.

27. Schmidt, W.G., *Metallic infiltration of reaction bonded silicon nitride.* Applied Sciences, 1983. **65**(Prog. Nitrogen Ceram.): p. 447-453.

28. Duffy, M.T., et al., *Development and evaluation of refractory CVD coatings as contact materials for molten silicon.* Journal of Crystal Growth, 1980. **50**(1): p. 347-365.

29. Nogi, K., *Measurements of thermophysical properties of semiconductors*, in *Outline of the Research and Development Results, JSUP 1997*. 1997: Tokyo. p. 119.

30. Li, J.G., *Wetting of ceramic materials by liquid silicon, aluminium and metallic melts containing titanium and other reactive elements: A review.* Ceramics International, 1994. **20**: p. 391-412.

31. Fitzer, E. and R. Gadow. *Investigationsof the reactivity of different carbons with liquid silicon*. in *Proceedings of the International Symposioum on Ceramic Components for Engines*. 1983. Tokyo, Japan: KTK Scientific Publishers.

32. Chiang, Y.-M., et al., *Reaction-formed silicon carbide.* Materials Science and Engineering A, 1991. **144**(1-2): p. 63-74.

33. Pampuch, R., E. Walasek, and J. Bialoskórski, *Reaction mechanism in carbon-liquid silicon systems at elevated temperatures.* Ceramics International, 1986. **12**(2): p. 99-106.

34. Hong, J.D., M.H. Hon, and R.F. Davis, *Self-diffusion in alpha and beta silicon carbide.* Ceramurgia International, 1979. **5**(4): p. 155-160.

35. Hauffe, K., *The mechanism of oxidation of metals and alloys at high temperatures.* Progress in Metal Physics, 1953. **4**: p. 71-104.